Journal of Nanobiotechnology

RESEARCH Open Access

A facile preparation of FePt-loaded few-layer MoS_2 nanosheets nanocomposites (F-MoS_2-FePt NCs) and their application for colorimetric detection of H_2O_2 in living cells

Zunfu Hu[1,2,3], Zhichao Dai[2], Xiaowei Hu[2], Baochan Yang[2,4], Qingyun Liu[4], Chuanhui Gao[1], Xiuwen Zheng[2*] and Yueqin Yu[1*]

Abstract

Background: Rapid and sensitive detection of H_2O_2 especially endogenous H_2O_2 is of great importance for series of industries including disease diagnosis and therapy. In this work, uniform FePt nanoparticles are successfully anchored onto Few-layer molybdenum disulfide nanosheets (F-MoS_2 NSs). The powder X-ray diffraction, transmission electron microscopy, UV–Vis spectra and atomic force microscopy were employed to confirm the structure of the obtained nanocomposites (F-MoS_2-FePt NCs). The prepared nanocomposites show efficient peroxidase-like catalytic activities verified by catalyzing the peroxidation substrate 4,4′-diamino-3,3′,5,5′-tetramethylbiphenyl (TMB) with the existence of H_2O_2.

Results: The optimal conditions of the constructed colorimetric sensing platform is proved as 35 °C and pH 4.2. Under optimal catalytic conditions, the detection limit for H_2O_2 detection reaches 2.24 μM and the linear ranger is 8 μM to 300 μM. Furthermore, the proposed colorimetric sensing platform was successfully utilized to detect the intracellular H_2O_2 of cancer cells (MCF-7).

Conclusions: These findings indicated that the F-MoS_2-FePt-TMB-H_2O_2 system provides a potential sensing platform for hydrogen peroxide monitoring in living cells.

Keywords: Few-layer MoS_2 nanosheets, FePt, Colorimetric, H_2O_2, Intracellular H_2O_2

Background

Hydrogen peroxide (H_2O_2) takes an essential position in many biochemical reactions, such as metabolism of proteins and carbohydrates. Furthermore, it can be used as a significant indicator of the occurrence of many serious disease especially cancer [1, 2]. Consequently, a sensitive, cost-effective, rapid and easy operation method for H_2O_2 determination would be demanded for bioassays and environmental applications [3]. Up to now, several techniques for H_2O_2 determination, such as chromatography [4], chemiluminescence, electrochemistry [5, 6] and colorimetric method [7], have been reported. Among these techniques, colorimetric route has several outstanding advantages, including visibility, low cost, easy automation, portability and operation convenience [8]. Although enormous progresses have been made, sensitive and rapid detection of H_2O_2 still remains highly need. Recently, due to its high selectivity, many nanomeaterials were employed to construct colorimetric sensors to detect H_2O_2.

Conventional enzymes are especially effective when catalyze series of reactions under mild conditions. However, conventional enzymes have rigorous limitations in practical use because they usually show insufficient

*Correspondence: zhengxiuwen@lyu.edu.cn; qustyu@163.com
[1] Collage of Chemistry and Molecular Engineering, Qingdao University of Science and Technology, Qingdao, China
[2] Key Laboratory of Functional Nanomaterials and Technology in Universities of Shandong, Linyi University, Linyi, China
Full list of author information is available at the end of the article

stability in cruel conditions, additionally, they are hard to purify and preserve [9]. Therefore, over the past few decades, an explosion of interests have been drawn to study enzyme-mimic materials aiming to get high efficiency without the mentioned shortcomings. To date, versatile nanomaterials, such as CoS NPs [10], Fe_3O_4 NPs [11, 12], Copper nanoclusters [7], metal–organic framework [13], WS_2 nanosheets [14], graphene oxide [15, 16], and kinds of metals [5, 17, 18] are used to fabricate nano-enzymes and exhibit effective catalytic activities suggesting prospective potentials in numerous bio-field, accompanied by series of advantages, including cost-effective, simple process, readily available raw materials, easy purification of products, low cost and long guarantee period [19, 20].

Molybdenum disulfide (MoS_2), with a graphene-like lamellar structure, is composed of S–Mo–S sandwich structure and held by weak van der Waals forces. The few-layer MoS_2 nanosheets (F-MoS_2 NSs) with excellent 2D structure possess a direct bandgap of 1.8 eV, which is much higher than the indirect bandgap in bulk MoS_2 NSs (1.2 eV) [21]. Hence, great efforts have been devoted to prepare few-layer MoS_2 NSs and they are applied in sensing, catalysis, supercapacitors and so on [22–27]. Furthermore, based on its super-large specific surface areas and abundant active edges, MoS_2 NSs have been utilized as base material to integrate with series of nanomaterials to further improve their catalytic performance [28]. A variety of monometallic nanoparticles (MNPs), such as Ag [29, 30], Pd [31], Pt [27], Au [32, 33] and Co NPs [34] have been successfully decorated on 2D MoS_2 NSs. The obtained MoS_2-MNPs can enhance their intrinsic properties. However, it is extremely difficult to further enhance the catalytic efficiency. Therefore, bimetallic nanoparticles (BNPs) were developed to improve the catalytic abilities [35–41].

Platinum-based BNPs have been widely used as sensing materials in non-enzymatic H_2O_2 sensing platforms and they show excellent electronic and catalytic properties. Until now, few attempts have been made to study the peroxidase-like catalytic ability of FePt NPs. Therefore, both MoS_2 and FePt NPs are expected to be employed together for the development of colorimetric sensor for H_2O_2 detection. In this work, few-layer MoS_2 NSs (F-MoS_2) loaded uniformly FePt NPs are prepared and the catalytic activity of the obtained NCs are systematically studied. Scheme 1 illustrates the technical route to prepare the NCs and the method to detect H_2O_2.

Results and discussion

Characterization of FePt nanoparticles, F-MoS_2 NSs and F-MoS_2-FePt NCs

The way to prepare F-MoS_2-FePt NCs is depicted in Scheme 1, while the experiments details are described in the experimental section. In this work, few-layer MoS_2

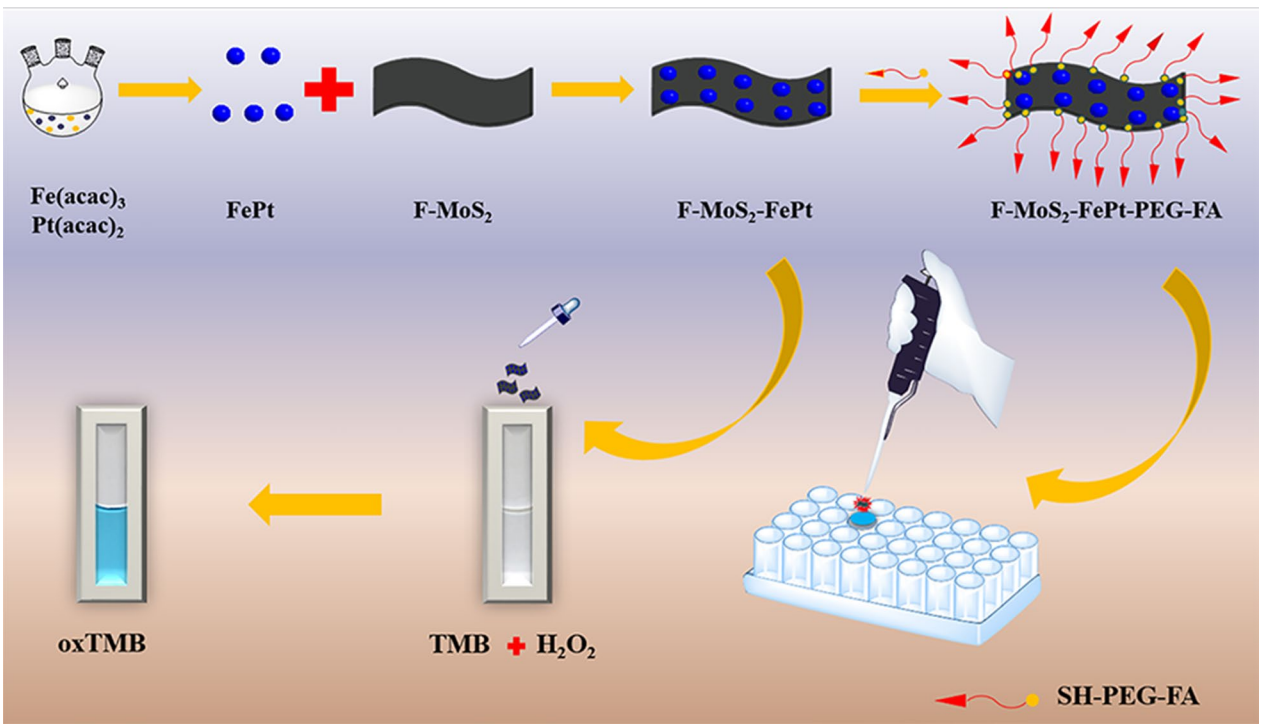

Scheme 1 Synthesis of few-layer MoS_2-FePt and schematic representation of the prepared colorimetric sensing platform for H_2O_2 detection in vivo

NSs (F-MoS_2) are obtained by exfoliating bulk MoS_2 via lithium intercalation–exfoliation. To investigate the thickness of the as-prepared MoS_2 NSs, atomic force microscopy (AFM) is utilized to measure as-prepared MoS_2 NSs. As shown in Additional file 1: Figure S1, the altitude of as-prepared MoS_2 NSs is around 2 nm, implying as-prepared MoS_2 NSs have 2–3 layers [25, 42].

Then TEM is employed to characterize the obtained nanomaterials. As illustrated in Fig. 1A, FePt NPs show uniform spherical morphology and the diameter is 4 nm. The lattice fringes of as-prepared FePt NPs can be seen obviously in Fig. 1B, the adjacent fringe spacing is about 0.224 nm, corresponding to the (111) lattice planes of FePt [43, 44]. To equally disperse FePt NPs on the surface of F-MoS_2 NSs, the obtained FePt NPs are firstly transformed from the organic phase to aqueous phase via ligand exchange. The zeta potential of FePt-DMSA is −25 mV, indicating the successful modification of FePt NPs by dimercaptosuccinic acid (DMSA) (Additional file 1: Figure S2). After modified with DMSA, FePt NPs can be well-dispersed in water. Then, the thiolated FePt NPs could be easily anchored on the defect-rich edge sites of F-MoS_2 NSs. As shown in Fig. 1C, FePt NPs are successfully anchored onto the surface of F-MoS_2 NSs. Bulk MoS_2 NSs are thicker and more visible than the exfoliated F-MoS_2 NSs, as shown in Additional file 1: Figure S3. The lattice fringe spacing of the loaded nanoparticles is also 0.224 nm, similar to the monodispersed FePt NPs, as illustrated in Fig. 1D.

Powder X-ray diffraction is utilized to further confirm the crystalline structure of as-prepared F-MoS_2 NSs, FePt NPs and F-MoS_2-FePt NCs. The data of X-ray diffraction are displayed in Fig. 2a. The exfoliated F-MoS_2 NSs exhibit series of highlighted peaks in accordance with the reported ultrathin MoS_2 nanosheets [33]. The XRD spectra of FePt NPs show four peaks in accordance with the reported FePt NPs [45]. Nearly all peaks of FePt NPs and F-MoS_2 NSs are found in the XRD patterns of F-MoS_2-FePt NCs, shown in Fig. 2a. All data show that F-MoS_2-FePt NCs are successfully prepared.

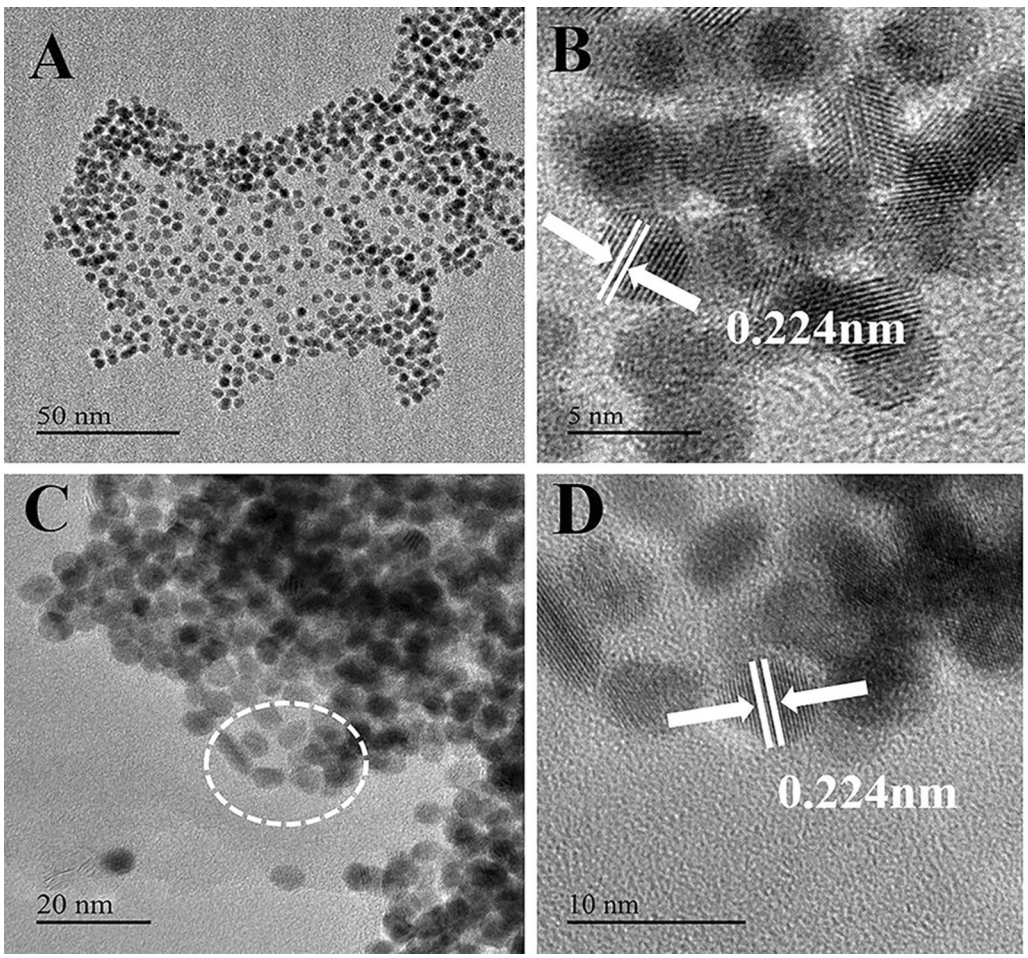

Fig. 1 TEM image of FePt NPs (**A**), HRTEM image of FePt NPs (**B**), TEM image of F-MoS_2-FePt (**C**) and HRTEM image of F-MoS_2-FePt (**D**)

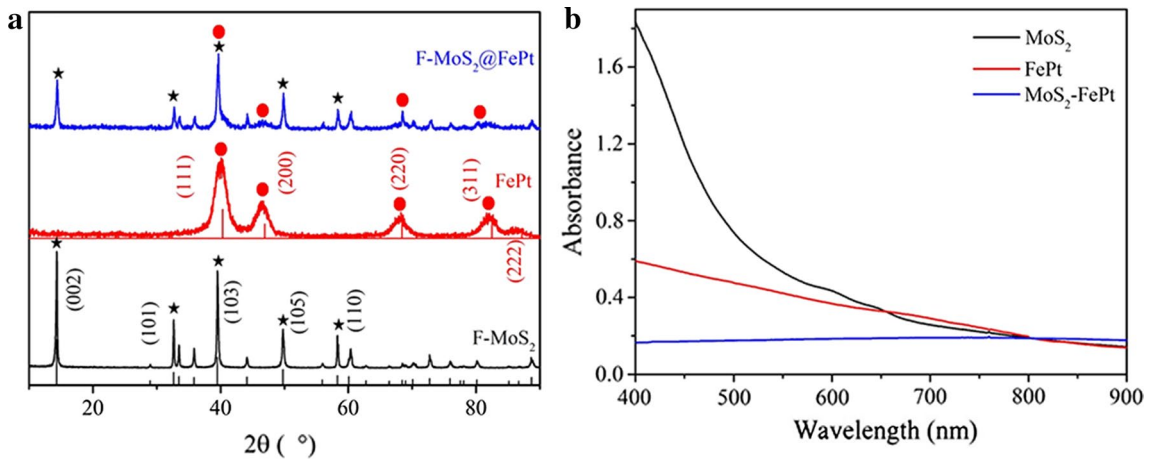

Fig. 2 **a** XRD patterns of MoS_2 (black line), FePt (red line) and F-MoS_2-FePt NCs (blue line). **b** UV–Vis spectra of MoS_2 (black line), FePt (red line) and F-MoS_2-FePt (blue line)

Furthermore, UV–Vis spectra are employed to characterize the obtained nanomaterials. As presented in Fig. 2b, after modified with FePt NPs, the strong absorbance of the exfoliated F-MoS_2 NSs is covered by sufficient FePt NPs, which show no obvious absorbance band from 400 to 900 nm. These results demonstrate that FePt NPs is successfully anchored on the surface of F-MoS_2 NSs.

Peroxidase-like activity of the obtained FePt, F-MoS_2 NSs and F-MoS_2-FePt NCs

To investigate the peroxidase-like catalytic activities of F-MoS_2-FePt NCs, 4,4′-diamino-3,3′,5,5′-tetramethylbiphenyl (TMB) is selected as chromogenic substrate to induce the color reaction. As depicted in Fig. 3A, a prominent absorption peak of the oxidation products at 652 nm is observed, while the other three systems do not have any well-developed peaks ranging from 400 to 800 nm. As shown in the inset of Fig. 3A, in the presence of F-MoS_2-FePt NCs and H_2O_2, the TMB solution turns blue promptly. However, the TMB solution remains colorless in the absence of either H_2O_2 or F-MoS_2-FePt NCs. As illustrated in Fig. 3B, the absorbance of F-MoS_2-FePt/TMB/H_2O_2 at 652 nm climbs rapidly and maintains constantly within 100 s, indicating TMB could be oxidized rapidly, while the absorbance of the reference experiment remains unchanged. The results prove that the obtained F-MoS_2-FePt NCs possess efficient peroxidase-like catalytic activity.

UV spectrum is utilized to estimate the catalytic activities of F-MoS_2-FePt NCs, bulk MoS_2 NSs, F-MoS_2 NSs and FePt NPs. As illustrated in Fig. 3C, the absorbance of F-MoS_2-FePt NCs reaches the highest value among all the materials. Moreover, the absorbance of F-MoS_2 NSs is much higher than bulk MoS_2 NSs, which is attributed to the higher specific surface area and more exposed active sites. Furthermore, the time-dependent mode of the UV–Vis spectra at 652 nm for these materials is also investigated. As depicted in Fig. 3D, the UV spectra of F-MoS_2-FePt NCs at 652 nm reach the balance within 100 s and the highest value is obtained, which indicates the strong synergistic effect between F-MoS_2 NSs and FePt NPs [46].

Similar to other enzyme-mimic systems, temperature and pH play vital roles in the catalytic activities of F-MoS_2-FePt NCs. As depicted in Fig. 4a, the absorption at 652 nm keeps relatively high between 20 and 50 °C and reaches the maximum value at about 40 °C. Similarly, the influence of the pH of the TMB solution is also investigated as the pH varies from 2.2 to 8. As depicted in Fig. 4b, higher UV–Vis absorption is acquired when the TMB solution is kept weakly acidic, which indicates that the weakly acidic environment would be beneficial to the oxidation of TMB. However, when the solution is kept neutral or basic, the UV–Vis absorption is relatively low, which is mainly attributed to the reason that under basic solution, more OH^- groups are absorbed on F-MoS_2-FePt NCs, occupying active sites of F-MoS_2-FePt NCs for the further reaction with H_2O_2 [47]. In summary, 35 °C and weakly acidic condition (pH = 4.2) are chosen as the optimum conditions.

Kinetic investigation of F-MoS_2-FePt NCs as peroxidase mimics

Under optimal conditions, TMB and H_2O_2 are chosen as the substrates to study the steady-state kinetic of the prepared F-MoS_2-FePt NCs. As illustrated in Fig. 5a, b, when TMB or H_2O_2 is catalyzed in certain concentration range, normative Michaels-Menten curves are acquired.

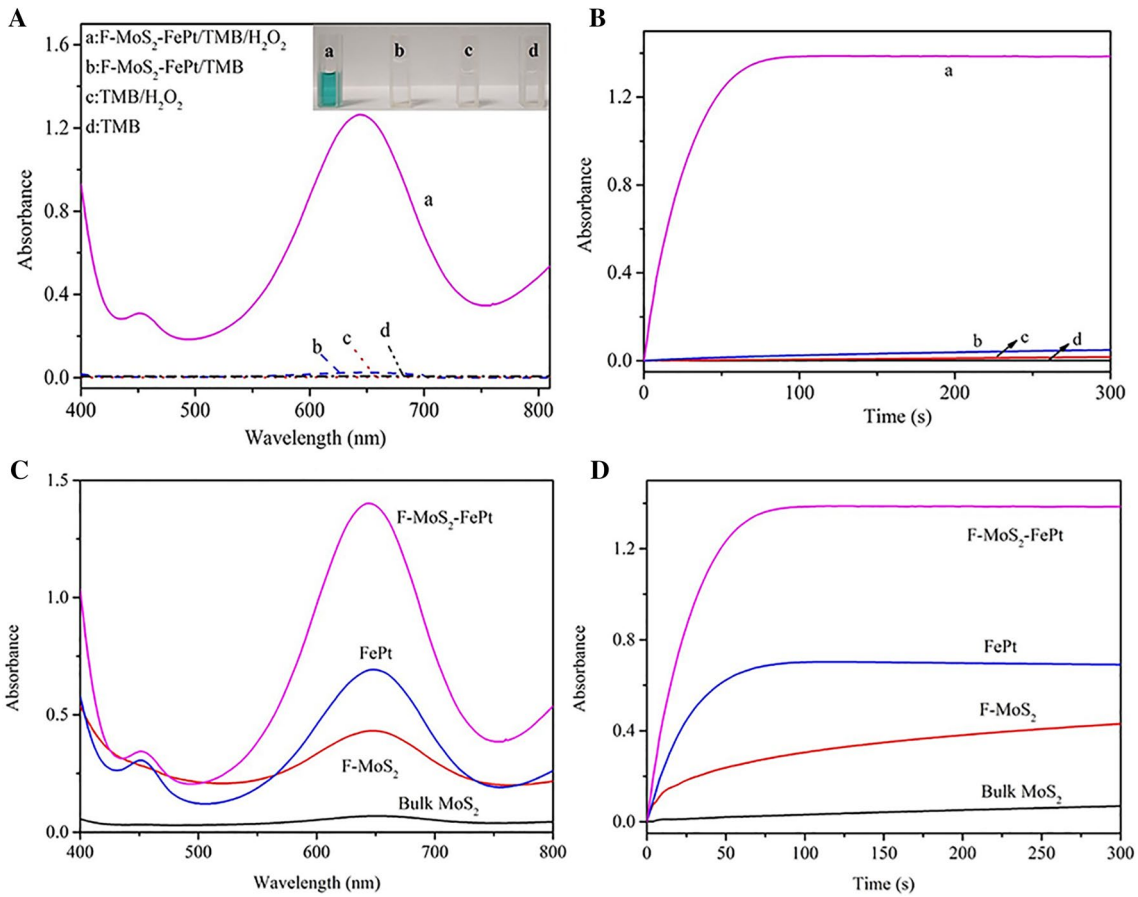

Fig. 3 **A** The investigation of peroxidase-like activity. (a) F-MoS_2-FePt NCs/H_2O_2/TMB; (b) F-MoS_2-FePt NCs/TMB; (c) H_2O_2/TMB; (d) TMB. **B** Time-dependent ultraviolet absorbance changes at 652 nm of these experiments. **C** The UV–Vis spectra of these obtained nano-enzymes. **D** Time-dependent ultraviolet absorbance changes at 652 nm of these obtained nano-enzymes

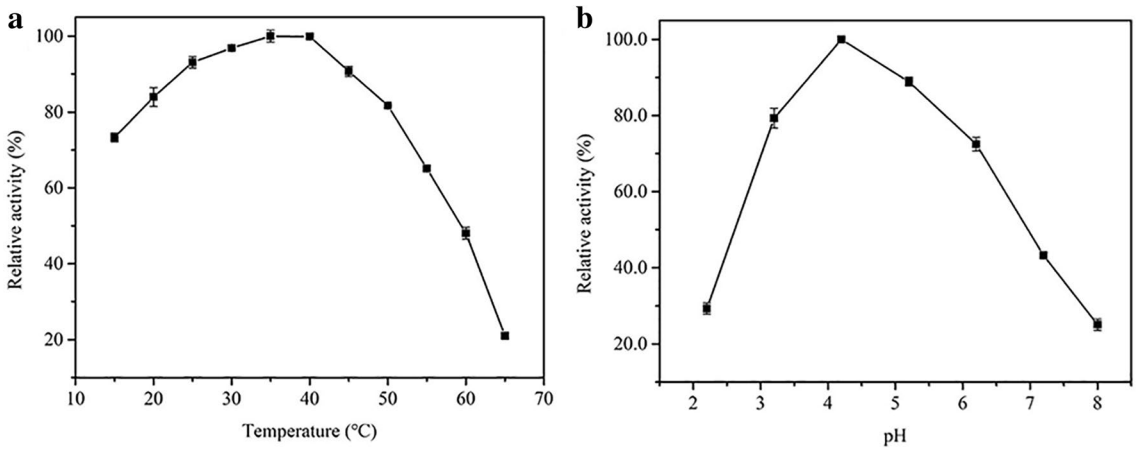

Fig. 4 The effects of temperature (**a**) and pH (**b**) on the catalytic activity of F-MoS_2-FePt NCs. The reaction conditions are shown as follows: 1.4 mL CPBS (pH 4.2), 200 μL TMB (1 mM), 200 μL F-MoS_2-FePt HNPs (20 μL mL^{-1}) and 200 μL H_2O_2 (0.25 M), the pH of the solution varies from 2.2 to 8

Michaels-Menten constant (K_m), which represents the affinity between substrates and catalyst, and the initial reaction velocity (V_{max}) are reckoned from the L-B plot, the results are displayed in Fig. 5c, d. Based on the calculation, for the obtained F-MoS_2-FePt NCs, the K_m value is 0.2225 mM and the relevant V_{max} is 2.9458×10^{-8} M s^{-1}.

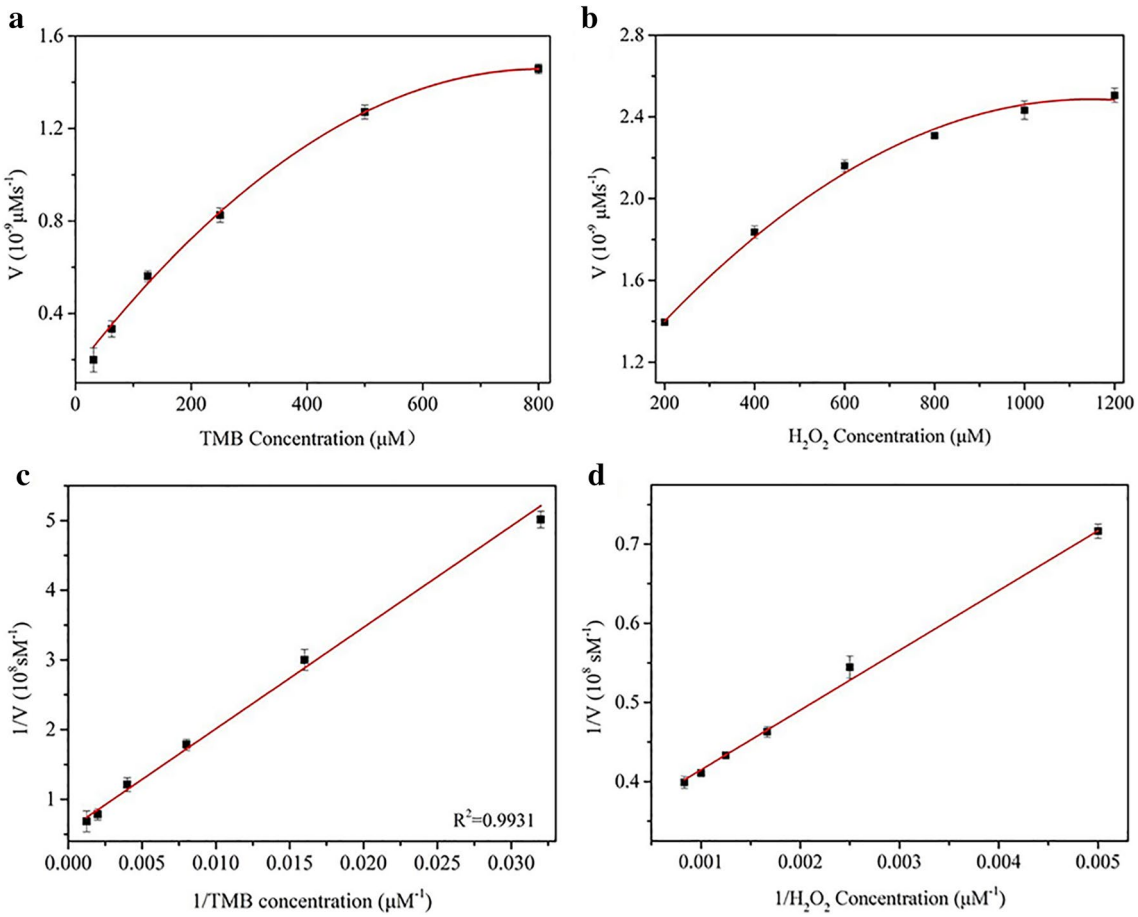

Fig. 5 Kinetic curves of F-MoS_2-FePt NCs. The concentration of TMB (**a**) and H_2O_2 (**b**) are varied. Double reciprocal plots F-MoS_2-FePt NCs by changing the concentration of TMB (**c**) and H_2O_2 (**d**)

Correspondingly, the K_m and V_{max} values with TMB are 0.4283 mM and 1.7857×10^{-8}M s^{-1}. Compared with other reported artificial enzymes and Horseradish peroxidase, the K_m and V_{max} are much smaller, which represents higher affinity between F-MoS_2-FePt NCs and the substrates (H_2O_2 and TMB) [40, 48–50].

Catalytic mechanism

Based on the prominent advantages such as cost-effective and high stability, p-Phthalic acid (TA) is applied to detect hydroxyl radicals (OH·) produced by the decomposition of H_2O_2. Fluorescence spectrometer is carried out to monitor the production generated from the combination of TA and hydroxide radical. As displayed in Fig. 6, as the amount of F-MoS_2-FePt NCs varies from 10 to 50 μg mL^{-1}, the fluorescence intensity decreases monotonically, which is caused by the reduction of hydroxide radical inhibited by high concentration of F-MoS_2-FePt NCs. According to the literatures, electron transfer mechanism is applied to explain these catalytic activities, as shows in Fig. 7 [51–53]. F-MoS_2-FePt NCs facilitate electrons shift between H_2O_2 and TMB. TMB can be easily absorbed on F-MoS_2-FePt NCs, this is because the higher affinity ($K_m = 0.4283$) and donated lone-pair electrons from the amino groups cause the increase of the electron density and mobility on the NCs, as a result, the electron transfer to H_2O_2 is facilitated and the oxidation of TMB is speed up [54].

Detection of H_2O_2 and sensing of the intracellular H_2O_2

The determination of H_2O_2 is carried out under the optimal conditions using UV–Vis absorption spectra ranging from 250 nm to 800 nm. As illustrated in Fig. 8a, with the increasing of H_2O_2 the UV absorption at 652 nm of the colorimetric system increases gradually. More importantly, the absorbance is in proportion to H_2O_2 concentration, providing a linear detection range from 8 to 300 μM (Fig. 8b). The corresponding image of the linear detection range of H_2O_2 is shown in the inset of Fig. 8a, which indicates that as the concentration decreases from

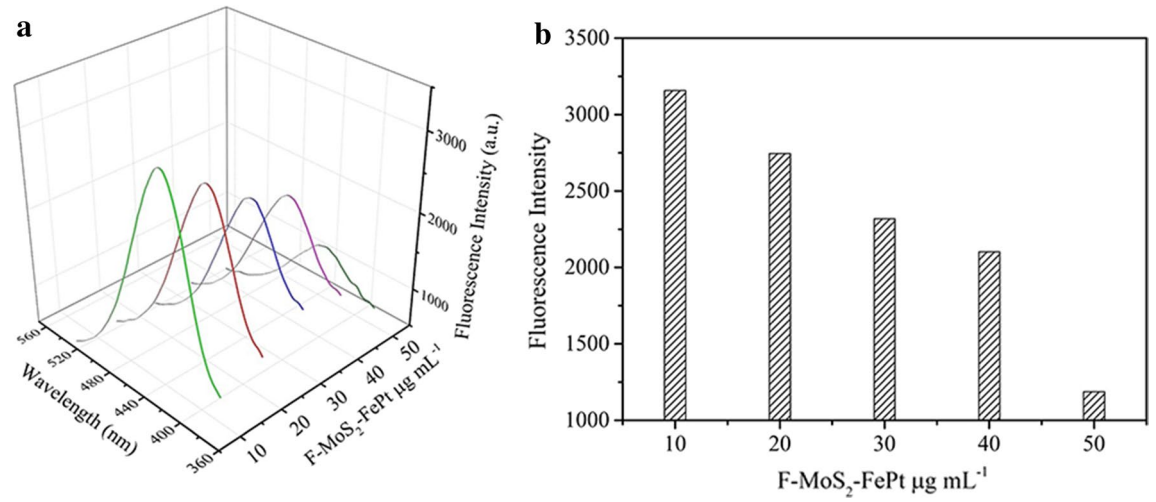

Fig. 6 **a** Emission spectra of the *p*-Phthalic acid with series of different amount of F-MoS_2-FePt NCs and constant concentration of H_2O_2. The reaction conditions are shown as follows: 5 mM TA, 0.25 M H_2O_2, along with different amount of F-MoS_2-FePt NCs. **b** The corresponding fluorescence intensity of different amount of F-MoS_2-FePt NCs

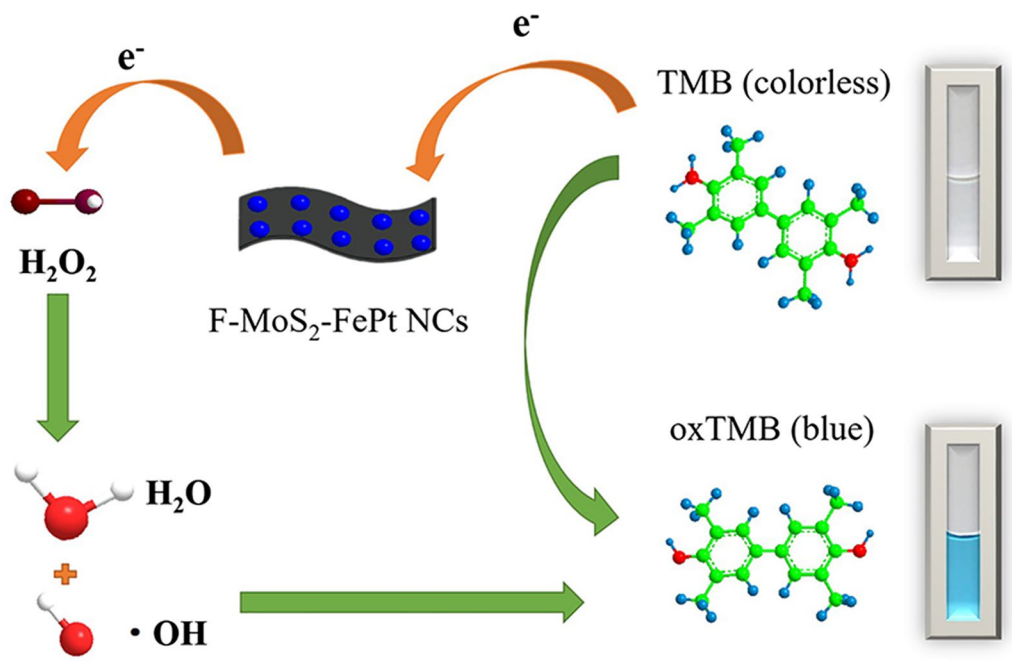

Fig. 7 The catalytic mechanism of the constructed F-MoS_2-FePt-TMB-H_2O_2 colorimetric sensing platform

300 to 8 μM, the color of these solution turns from dark blue to baby blue, the detection limit is reckoned to be 2.24 μM. When compared with other nanomaterials-based colorimetric sensing platforms the linear detection range of the constructed sensing platform (F-MoS_2-FePt-TMB-H_2O_2) is more wide and a lower limit of detection is obtained, as listed in Additional file 1: Table S1 [48, 50, 55, 56].

To verify the feasibility of the detection of H_2O_2 in living cells, the obtained sensing platform is utilized to detect the intracellular H_2O_2. To improve the stability in the culture medium, the obtained NCs is modified with SH-PEG-FA. Then the established colorimetric sensing platform is further utilized to detect the intracellular H_2O_2 in MCF-7. After 4 h' co-incubation with F-MoS_2-FePt-PEG-FA, 0.2 mM TMB and 100 μM H_2O_2 are added

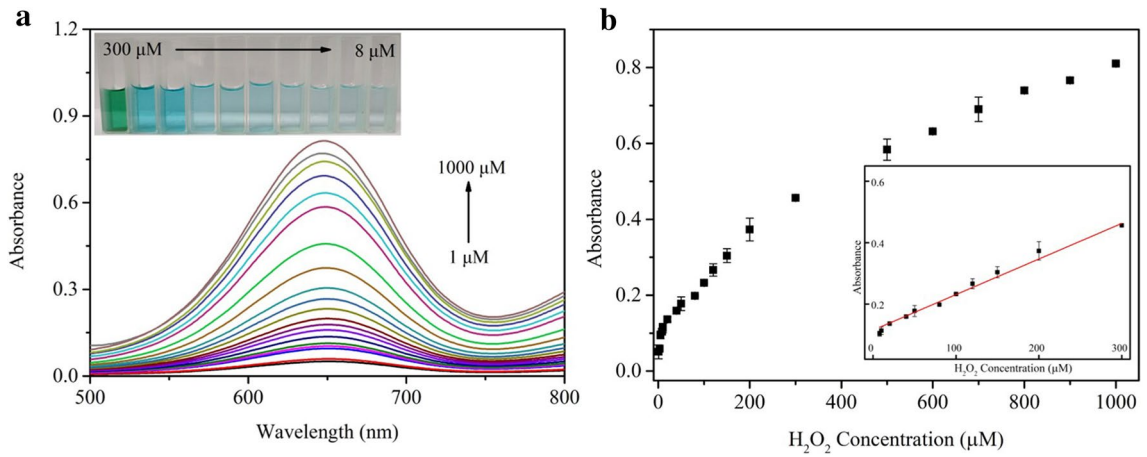

Fig. 8 **a** The absorption spectra of H_2O_2 with various concentration and the corresponding images are shown in the inset picture. These experiments conditions are shown as follows: 1.4 mL CPBS (pH 4.2), 200 μL TMB (1 mM), 200 μL F-MoS_2-FePt HNPs (20 μg mL^{-1}) and different amount of H_2O_2. **b** Dose–response curve for H_2O_2 determination

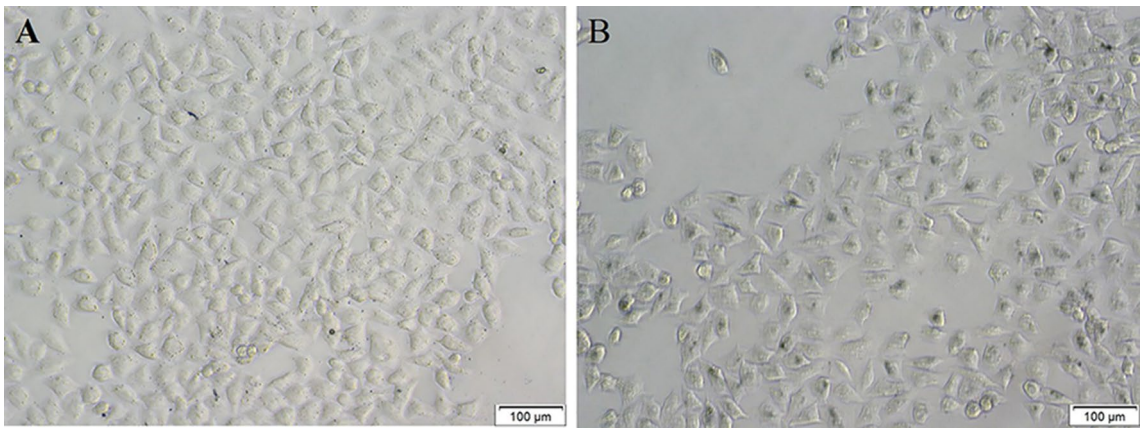

Fig. 9 Images of MCF-7 incubated with F-MoS_2-FePt-PEG-FA NCs and TMB (**A**) F-MoS_2-FePt-PEG-FA and TMB and H_2O_2 (**B**)

into the plate and incubated for another 40 min. After co-incubation the cells are subjected to the electron microscope and the images are shown in Fig. 8. Compared with the cells only treated with NCs and TMB (Fig. 9A), the MCF-7 cells treated with NCs, TMB and H_2O_2 turn to clear blue (Fig. 9B). Without FA receptor on the cell membrane of normal cell (L02), nearly none NCs can be endocytosed (Additional file 1: Figure S5B). When treated with TMB only, MCF-7 remains colorless, as depicted in Additional file 1: Figure S5 A. The sensitive and selective of intracellular detection indicates that the F-MoS_2-FePt-PEG-FA have the potential for monitoring of H_2O_2 in living cells.

Conclusion

In this work, a sensitive and rapid colorimetric sensing platform for H_2O_2 detection utilizing F-MoS_2-FePt NCs as artificial enzyme is constructed. The uniformly prepared FePt NPs are anchored on the surface of exfoliated few-layer MoS_2 NSs by a facile operation. Series of experiments are carried out to verify the peroxidase-like catalytic activity of the obtained NCs. Under optimal conditions, the linear range of H_2O_2 detection is between 8 and 300 μM and the detection limit is 2.24 μM. Compared with other reported methods, F-MoS_2-FePt NCs-based colorimetric sensing platform for H_2O_2 detection is a sensitive, simple and cost-effective method. To improve the stability and transmembrane performance of F-MoS_2-FePt NCs, the surface of the prepared NCs is modified by SH-PEG-FA for intracellular H_2O_2 detection, which indicates that the sensor could be applied in living

cells testing and has potential in disease diagnosis and therapy.

Additional file

Additional file 1: Figure S1. The atomic force microscopy (AFM) images of the as-prepared Few-layers MoS_2 nanosheets. **Figure S2.** The potential distribution of FePt-DMSA NPs. **Figure S3. a** TEM image of bulk MoS_2 sheets; **b** HRTEM of MoS_2-FePt. **Figure S4.** Image of FePt NPs before and after transferred from lipophilic to hydrophilic by DMSA via ligand exchange reaction. For the two phases, the upper layer is n-hexane, the lower is the water. **Figure S5. a** Images of MCF-7 cells incubated with TMB (1 mM) and **b** L02 cells incubated with F-MoS_2-FePt-PEG-FA and TMB (1 mM). **Table S1.** Comparison of the linear range and the detection limit of H_2O_2 by means of different sensors.

Authors' contributions

ZH performed experiments; ZD, XH, BY and QL drew the TOC, scheme and figures, YY wrote the paper with support from XZ. All authors contributed to the general discussion. All authors read and approved the final manuscript.

Author details

[1] Collage of Chemistry and Molecular Engineering, Qingdao University of Science and Technology, Qingdao, China. [2] Key Laboratory of Functional Nanomaterials and Technology in Universities of Shandong, Linyi University, Linyi, China. [3] School of Materials Science and Engineering, Linyi University, Linyi 276000, China. [4] School of Chemistry and Environmental Engineering, Shandong University of Science and Technology, Qingdao 266510, People's Republic of China.

Acknowledgements

Financial support from the National Natural Science Foundation of China (Grant Nos.: 21675073, 51872150), Primary Research and Development Plan of Shandong Province (2017GGX20115) and Shandong Province Natural Science Foundation (Nos.: ZR2017BB070, ZR2018MB034) are gratefully acknowledged.

Competing interests

The authors declare that they have no competing interests.

Availability of data and materials

All data generated or analyzed during this study are included in the article and Additional file.

Consent for publication

Not applicable.

Ethics approval and consent to participate

Not applicable.

Studies involving human participants, human data or human tissue

Not applicable.

Publisher's Note

Received: 6 September 2018 Accepted: 11 February 2019
Published online: 13 March 2019

References

1. Zhu J, Wang S. In situ growth of copper oxide-graphite carbon nitride nanocomposites with peroxidase-mimicking activity for electrocatalytic and colorimetric detection of hydrogen peroxide. Carbon. 2018;129:29–37.
2. Ranji-Burachaloo H, Karimi F, Xie K, Fu Q, Gurr PA, Dunstan DE, Qiao GG. MOF-mediated destruction of cancer using the cell's own hydrogen peroxide. ACS Appl Mater Interfaces. 2017;9:33599–608.
3. Zhan T, Kang J, Li X, Pan L, Li G, Hou W. NiFe layered double hydroxide nanosheets as an efficiently mimic enzyme for colorimetric determination of glucose and H_2O_2. Sensor Actuators B Chem. 2018;255:2635–42.
4. Zou J, Shen M, Zhang M, Tu M, Feng R, Yan Y, Zou B. An improved reference method for serum cations measurement by ion chromatography. J Clin Lab Anal. 2018;32:22429–35.
5. Zhang C, Zhang R, Gao X, Cheng C, Hou L, Li X, Chen W. Small naked Pt nanoparticles confined in mesoporous shell of hollow carbon spheres for high-performance nonenzymatic sensing of H_2O_2 and glucose. ACS Omega. 2018;3:96–105.
6. Lin X, Ni Y, Kokot S. Electrochemical cholesterol sensor based on cholesterol oxidase and MoS_2 -AuNPs modified glassy carbon electrode. Sensor Actuators B Chem. 2016;233:100–6.
7. Dutta AK, Das S, Samanta S, Samanta PK, Adhikary B, Biswas P. CuS nanoparticles as a mimic peroxidase for colorimetric estimation of human blood glucose level. Talanta. 2013;107:361–7.
8. Chen Q, Chen H, Li Z, Pang J, Lin T, Guo L, Fu F. Colorimetric sensing of glyphosate in environmental water based on peroxidase mimetic activity of MoS_2 nanosheets. J Nanosci Nanotechnol. 2017;17:5730–4.
9. Wang Y, Zhang D, Wang J. Metastable alpha-$AgVO_3$ microrods as peroxidase mimetics for colorimetric determination of H_2O_2. Mikrochim Acta. 2017;185:1–8.
10. Yang H, Zha J, Zhang P, Xiong Y, Su L, Ye F. Sphere-like CoS with nanostructures as peroxidase mimics for colorimetric determination of H_2O_2 and mercury ions. RSC Adv. 2016;6:66963–70.
11. Wei H, Wang E. Fe_3O_4 magnetic nanoparticles as peroxidase mimetics and their applications in H_2O_2 and glucose detection. Anal Chem. 2008;80:2250–4.
12. Ma Y, Zhang Z, Ren C, Liu G, Chen X. Fe_3O_4 magnetic nanoparticles as peroxidase mimetics and their applications in H_2O_2 and glucose detection. Analyst. 2012;137:485–9.
13. Tang XQ, Zhang YD, Jiang ZW, Wang DM, Huang CZ, Li YF. Fe_3O_4 and metal-organic framework MIL-101(Fe) composites catalyze luminol chemiluminescence for sensitively sensing hydrogen peroxide and glucose. Talanta. 2018;179:43–50.
14. Khataee A, Irani-nezhad MH, Hassanzadeh J, Joo SW. Superior peroxidase mimetic activity of tungsten disulfide nanosheets/silver nanoclusters composite: colorimetric, fluorometric and electrochemical studies. J Colloid Interface Sci. 2018;515:39–49.
15. Fu Y, Huang D, Li C, Zou L, Ye B. Graphene blended with SnO_2 and Pd-Pt nanocages for sensitive non-enzymatic electrochemical detection of H_2O_2 released from living cells. Anal Chim Acta. 2018;1014:10–8.
16. Lin L, Song X, Chen Y, Rong M, Zhao T, Wang Y, Jiang Y, Chen X. Intrinsic peroxidase-like catalytic activity of nitrogen-doped graphene quantum dots and their application in the colorimetric detection of H_2O_2 and glucose. Anal Chim Acta. 2015;869:89–95.
17. Shi L, Layani M, Cai X, Zhao H, Magdassi S, Lan M. An inkjet printed Ag electrode fabricated on plastic substrate with a chemical sintering approach for the electrochemical sensing of hydrogen peroxide. Sensor Actuators B Chem. 2018;256:938–45.
18. Jin L, Meng Z, Zhang Y, Cai S, Zhang Z, Li C, Shang L, Shen Y. Ultrasmall Pt nanoclusters as robust peroxidase mimics for colorimetric detection of glucose in human serum. ACS Appl Mater Interfaces. 2017;9:10027–33.
19. Singh VK, Yadav PK, Chandra S, Bano D, Talat M, Hasan SH. Peroxidase mimetic activity of fluorescent NS-carbon quantum dots and its application for colorimetric detection of H_2O_2 and glutathione in human blood serum. J Mater Chem B. 2018;42:6803–9.
20. Yang Q, Lu S, Shen B, Bao S, Liu Y. An iron hydroxyl phosphate microoctahedron catalyst as an efficient peroxidase mimic for sensitive and colorimetric quantification of H_2O_2 and glucose. New J Chem. 2018;42:6803–9.
21. Zhu C, Zeng Z, Li H, Li F, Fan C, Zhang H. Single-layer MoS_2-based nanoprobes for homogeneous detection of biomolecules. J Am Chem Soc. 2013;135:5998–6001.
22. Zhao K, Gu W, Zheng S, Zhang C, Xian Y. SDS-MoS_2 nanoparticles as highly-efficient peroxidase mimetics for colorimetric detection of H_2O_2 and glucose. Talanta. 2015;141:47–52.

23. Wang R, Jin D, Zhang Y, Wang S, Lang J, Yan X, Zhang L. Engineering metal organic framework derived 3D nanostructures for high performance hybrid supercapacitors. J Mater Chem A. 2017;5:292–302.
24. Yin W, Yu J, Lv F, Yan L, Zheng LR, Gu Z, Zhao Y. Functionalized nano-MoS_2 with peroxidase catalytic and near-infrared photothermal activities for safe and synergetic wound antibacterial applications. ACS Nano. 2016;10:11000–11.
25. Meng X, Liu Z, Cao Y, Dai W, Zhang K, Dong H, Feng X, Zhang X. Fabricating aptamer-conjugated PEGylated-MoS_2/$Cu_{1.8}S$ theranostic nanoplatform for multiplexed imaging diagnosis and chemo-photothermal therapy of cancer. Adv Funct Mater. 2017;27:1605592.
26. Zhou W, Yin Z, Du Y, Huang X, Zeng Z, Fan Z, Liu H, Wang J, Zhang H. Synthesis of few-layer MoS_2 nanosheet-coated TiO_2 nanobelt heterostructures for enhanced photocatalytic activities. Small. 2013;9:140–7.
27. Cai S, Han Q, Qi C, Wang X, Wang T, Jia X, Yang R, Wang C. MoS_2-Pt_3Au_1 nanocomposites with enhanced peroxidase-like activities for selective colorimetric detection of phenol. Chin J Chem. 2017;35:605–12.
28. Zhu D, Liu W, Zhao D, Hao Q, Li J, Huang J, Shi J, Chao J, Su S, Wang L. Label-free electrochemical sensing platform for microRNA-21 detection using thionine and gold nanoparticles co-functionalized MoS_2 nanosheet. ACS Appl Mater Interfaces. 2017;41:35597–603.
29. Wu X, Yan X, Dai Y, Wang J, Wang J, Cheng X. Facile synthesis of AgNPs/MoS_2 nanocomposite with excellent electrochemical properties. Mater Lett. 2015;152:128–30.
30. Zu S, Li B, Gong Y, Li Z, Ajayan PM, Fang Z. Active control of plasmon-exciton coupling in MoS_2-Ag hybrid nanostructures. Adv Opt Mater. 2016;4:1463–9.
31. Yuwen L, Xu F, Xue B, Luo Z, Zhang Q, Bao B, Su S, Weng L, Huang W, Wang L. General synthesis of noble metal (Au, Ag, Pd, Pt) nanocrystal modified MoS_2 nanosheets and the enhanced catalytic activity of Pd–MoS_2 for methanol oxidation. Nanoscale. 2014;6:5762–9.
32. Su S, Zou M, Zhao H, Yuan C, Xu Y, Zhang C, Wang L, Fan C, Wang L. Shape-controlled gold nanoparticles supported on MoS_2 nanosheets: synergistic effect of thionine and MoS_2 and its application for electrochemical label-free immunosensing. Nanoscale. 2015;7:19129–35.
33. Nirala NR, Prakash R. One step synthesis of AuNPs@MoS_2-QDs composite as a robust peroxidase- mimetic for instant unaided eye detection of glucose in serum, saliva and tear. Sens Actuators B Chem. 2018;263:109–19.
34. Zhu Z, Yin H, He CT, Al-Mamun M, Liu P, Jiang L, Zhao Y, Wang Y, Yang HG, Tang Z, Wang D, Chen XM, Zhao H. Ultrathin transition metal dichalcogenide/3d metal hydroxide hybridized nanosheets to enhance hydrogen evolution activity. Adv Mater. 2018;30:1801171.
35. Liu W, Ding F, Wang Y, Mao L, Liang R, Zou P, Wang X, Zhao Q, Rao H. Fluorometric and colorimetric sensor array for discrimination of glucose using enzymatic-triggered dual-signal system consisting of Au@Ag nanoparticles and carbon nanodots. Sensor Actuators B Chem. 2018;265:310–7.
36. Liu W, Hiekel K, Hübner R, Sun H, Ferancova A, Sillanpää M. Pt and Au bimetallic and monometallic nanostructured amperometric sensors for direct detection of hydrogen peroxide: influences of bimetallic effect and silica support. Sens Actuators B Chem. 2018;255:1325–34.
37. Chen Q, Lin T, Huang J, Chen Y, Guo L, Fu F. Colorimetric detection of residual hydrogen peroxide in soaked food based on Au@Ag nanorods. Anal Methods. 2018;10:504–7.
38. Bai Z, Dong W, Ren Y, Zhang C, Chen Q. Preparation of nano Au and Pt alloy microspheres decorated with reduced graphene oxide for nonenzymatic hydrogen peroxide sensing. Langmuir. 2018;34:2235–44.
39. Cai S, Jia X, Han Q, Yan X, Yang R, Wang C. Porous Pt/Ag nanoparticles with excellent multifunctional enzyme mimic activities and antibacterial effects. Nano Res. 2017;10:2056–69.
40. Zhang XZ, Zhou Y, Zhang W, Zhang Y, Gu N. Polystyrene@Au@prussian blue nanocomposites with enzyme-like activity and their application in glucose detection. Colloids Surf A. 2016;490:291–9.
41. Liu H, Jiao M, Gu C, Zhang M. Au@$CuxO_S$ yolk-shell nanomaterials with porous shells act as a new peroxidase mimic for the colorimetric detection of H_2O_2. J Alloys Compd. 2018;741:197–204.
42. Yin W, Yan L, Yu J, Tian G, Zhou L, Zheng X, Zhang X, Yong Y, Li J, Gu Z, Zhao Y. High-throughput synthesis of single-layer MoS_2 nanosheets as a near-infrared photothermal-triggered drug delivery for effective cancer therapy. ACS Nano. 2014;20:6922–33.
43. Wang C, Hou Y, Kim J, Sun S. A general strategy for synthesizing FePt nanowires and nanorods. Angew Chem Int Ed. 2007;46:6333–5.
44. Chen M, Liu JP, Sun S. One-step synthesis of FePt nanoparticles with tunable size. J Am Chem Soc. 2004;126:8394–5.
45. Kim J, Lee Y, Sun S. Structurally ordered FePt nanoparticles and their enhanced catalysis for oxygen reduction reaction. J Am Chem Soc. 2010;132:4996–7.
46. Xing M, Xu W, Dong C, Bai Y, Zeng J, Zhou Y, Zhang J, Yin Y. Metal sulfides as excellent Co-catalysts for H_2O_2 decomposition in advanced oxidation processes. Chem. 2018;4:1359–72.
47. Chen X, Su B, Cai Z, Chen X, Oyama M. PtPd nanodendrites supported on graphene nanosheets: a peroxidase-like catalyst for colorimetric detection of H_2O_2. Sens Actuators B Chem. 2014;201:286–92.
48. Cai S, Han Q, Qi C, Lian Z, Jia X, Yang R, Wang C. $Pt_{74}Ag_{26}$ nanoparticles-decorated ultrathin MoS_2 nanosheets as novel peroxidase mimics for highly selective colorimetric detection of H_2O_2 and glucose. Nanoscale. 2016;8:3685–94.
49. Liu F, He J, Zeng M, Hao J, Guo Q, Song Y, Wang L. Cu–hemin metal-organic frameworks with peroxidase-like activity as peroxidase mimics for colorimetric sensing of glucose. J Nanopart Res. 2016;18:106–14.
50. Wang N, Sun J, Chen L, Fan H, Ai S. A $Cu_2(OH)_3Cl$-CeO_2 nanocomposite with peroxidase-like activity, and its application to the determination of hydrogen peroxide, glucose and cholesterol. Microchim Acta. 2015;182:1733–8.
51. Wang Q, Zhang L, Shang C, Zhang Z, Dong S. Triple-enzyme mimetic activity of nickel-palladium hollow nanoparticles and their application in colorimetric biosensing of glucose. Chem Commun (Camb). 2016;52:5410–3.
52. Mu J, Zhang L, Zhao M, Wang Y. Catalase mimic property of Co_3O_4 nanomaterials with different morphology and its application as a calcium sensor. ACS Appl Mater Interfaces. 2014;6:7090–8.
53. Ding Y, Yang B, Liu H, Liu Z, Zhang X, Zheng X, Liu Q. FePt-Au ternary metallic nanoparticles with the enhanced peroxidase-like activity for ultrafast colorimetric detection of H_2O_2. Sens Actuators B Chem. 2018;259:775–83.
54. Zhu L, Gao F, Ge J. *N,N'*-di-caboxy methyl perylene diimides functionalized magnetic nanocomposites with enhanced peroxidase-like activity for colorimetric sensor of H_2O_2 and glucose. Sens Actuators B Chem. 2016;41:5853–62.
55. Liu H, Ding Y, Yang B, Liu Z, Liu Q, Zhang X. Colorimetric and ultrasensitive detection of H_2O_2 based on Au/Co_3O_4-CeOx nanocomposites with enhanced peroxidase-like performance. Sens Actuators B Chem. 2018;271:336–45.
56. Liu Q, Yang Y, Lv X, Ding Y, Zhang Y, Jing J, Xu C. One-step synthesis of uniform nanoparticles of porphyrin functionalized ceria with promising peroxidase mimetics for H_2O_2 and glucose colorimetric detection. Sens Actuators B Chem. 2017;240:726–34.